Discrepancies in temporal *p*CO_2 variability from Earth System Models and *p*CO_2-products

Christopher Danek & Judith Hauck

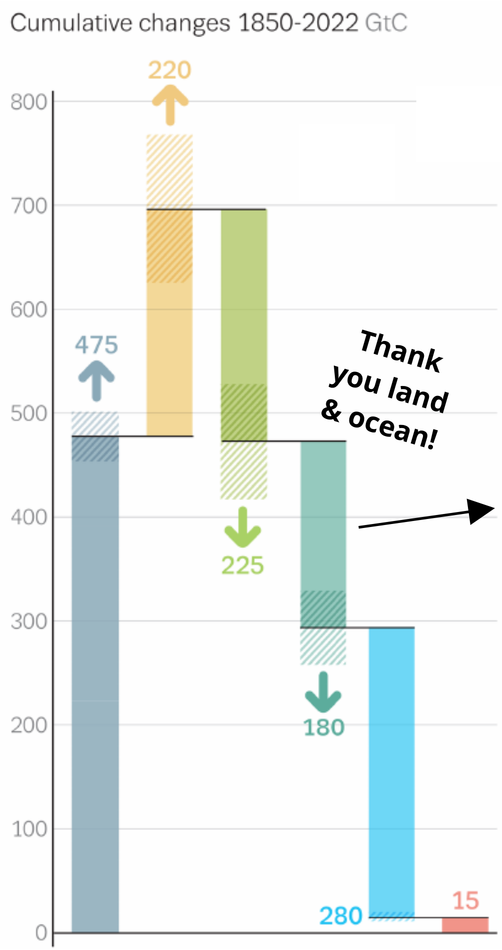

Global Carbon Budget (Friedlingstein et al. 2023)

→ oceans took up ~26% of total anthropogenic carbon emissions since 1850

$$f_{\text{sea-air}} = (\text{pCO}_{2,\text{sw}} - \text{pCO}_{2,\text{air}}) \times K_w \times (1 - f_{\text{ice}}) \times K_0$$

ALFRED-WEGENER-INSTITUT
HELMHOLTZ-ZENTRUM FÜR POLAR- UND MEERESFORSCHUNG

Discrepancies in temporal pCO_2 variability from Earth System Models and pCO_2-products

Christopher Danek & Judith Hauck

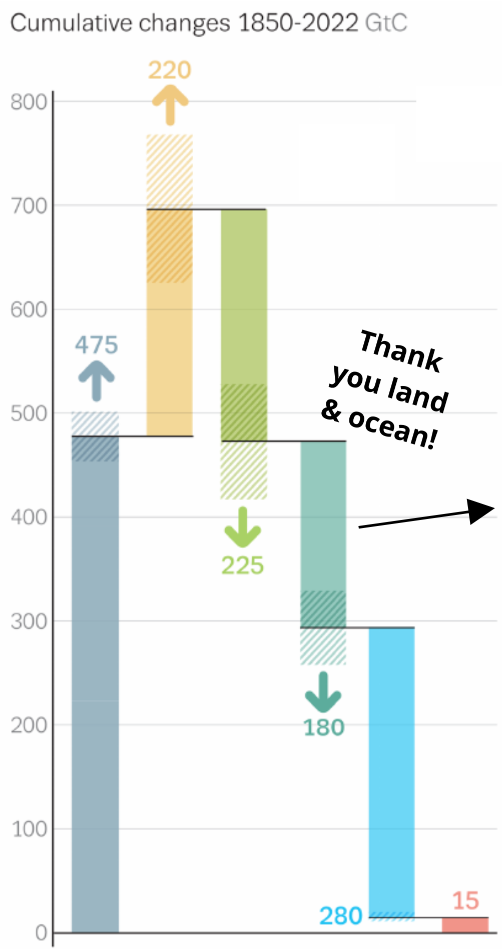

Global Carbon Budget (Friedlingstein et al. 2023)

→ oceans took up ~26% of total anthropogenic carbon emissions since 1850

$$f_{\text{sea-air}} = (\text{pCO}_{2,\text{sw}} - \text{pCO}_{2,\text{air}}) \times K_w \times (1 - f_{\text{ice}}) \times K_0$$

→ systematic model biases in FCO_2 mean/trend/variability

→ carbon-climate feedbacks in our changing world?

→ pCO_2 in Earth System Models (ESMs)?

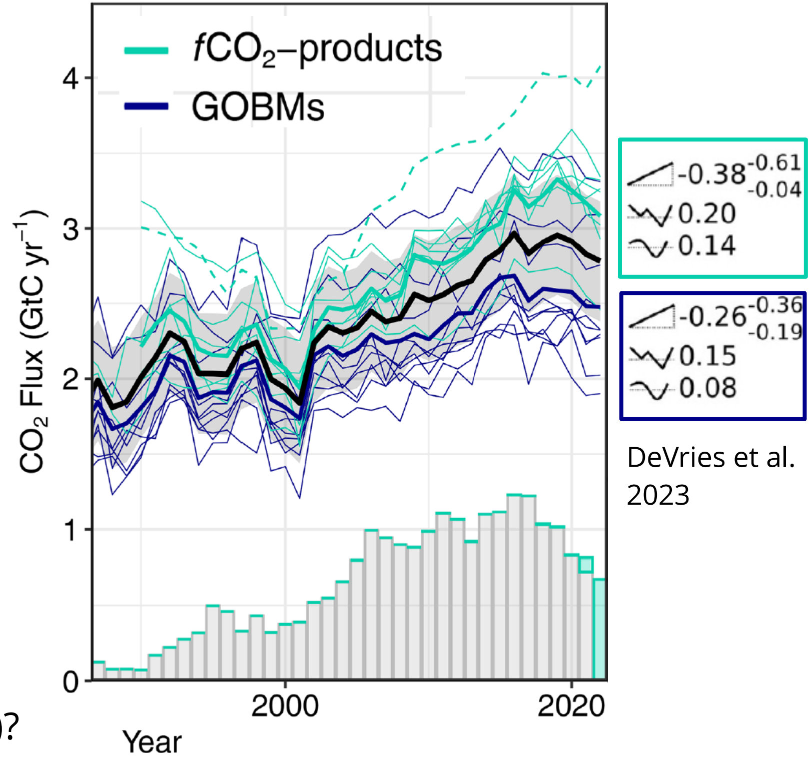

DeVries et al. 2023

ALFRED-WEGENER-INSTITUT
HELMHOLTZ-ZENTRUM FÜR POLAR- UND MEERESFORSCHUNG

pCO$_2$-product **SeaFlux** (Gregor and Fay 2021)

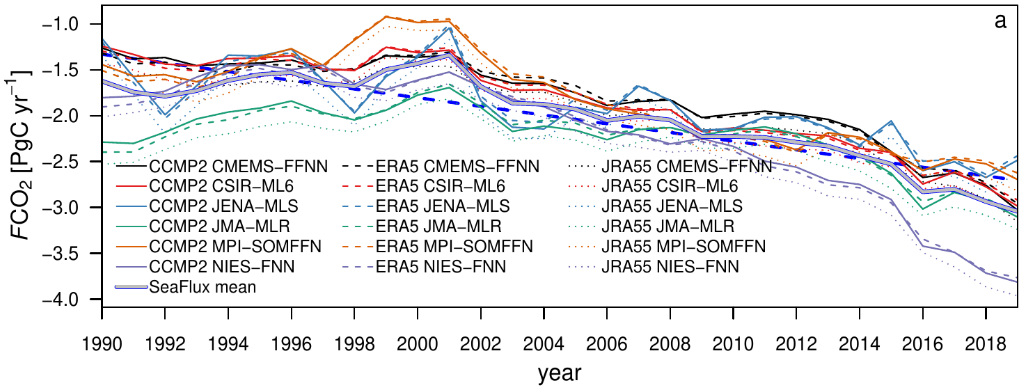

$$f_{\text{sea-air}} = K_w \times (1 - f_{\text{ice}}) \times K_0 \times (\text{pCO}_{2,\text{sw}} - \text{pCO}_{2,\text{air}})$$

CMIP6 models & AWI-ESM-1-REcoM

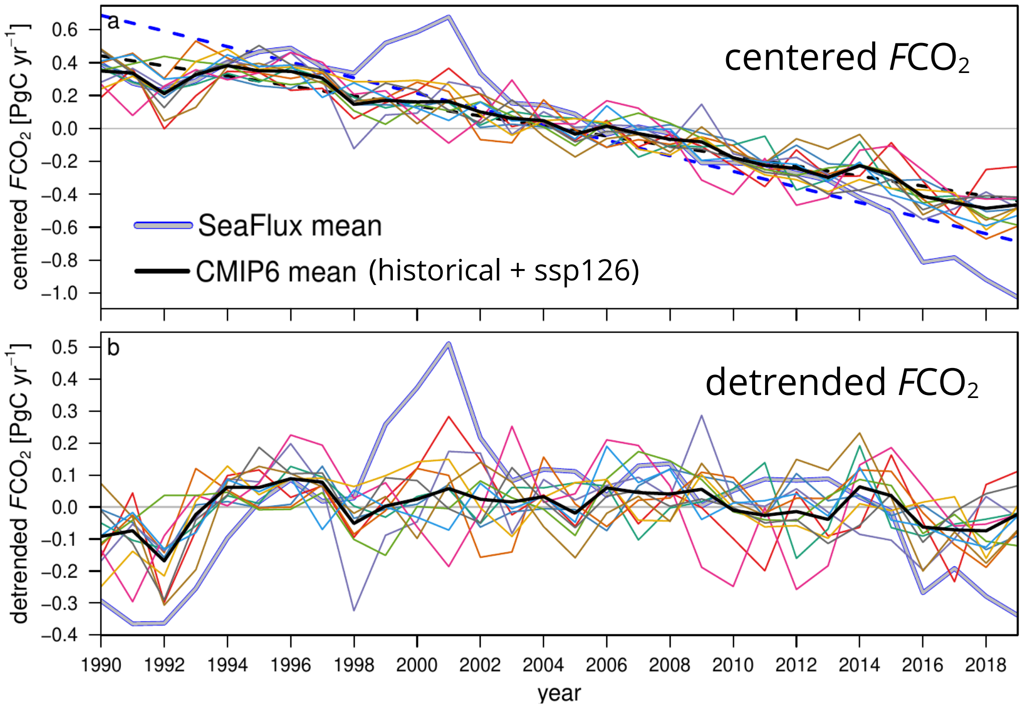

→ focus on temporal variability: center/detrend

→ FCO_2 weakening (1990s), reinvigoration (after 2000) and latest increase missing in CMIP6

ALFRED-WEGENER-INSTITUT
HELMHOLTZ-ZENTRUM FÜR POLAR-
UND MEERESFORSCHUNG

pCO_2-product **SeaFlux** (Gregor and Fay 2021)

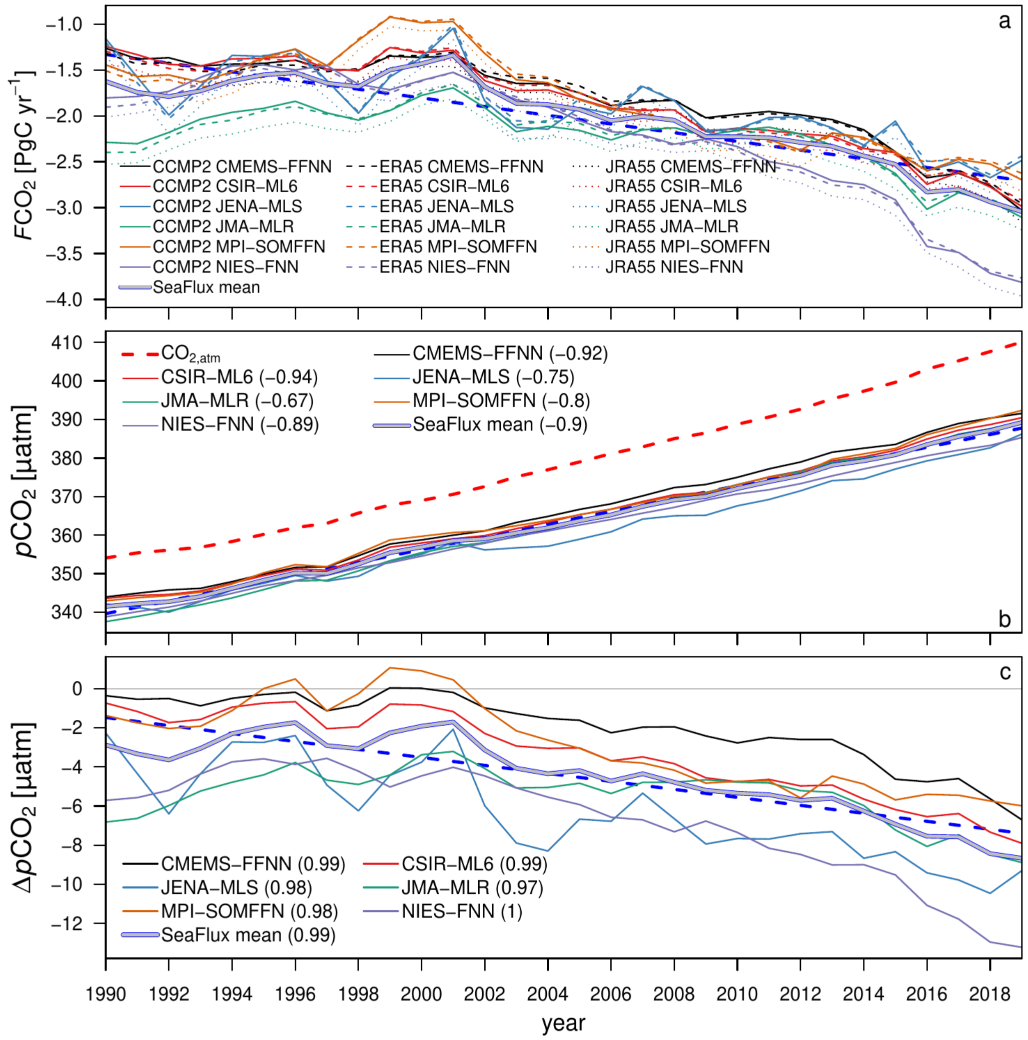

$$f_{\text{sea-air}} = K_w \times (1 - f_{\text{ice}}) \times K_0 \times (\text{pCO}_{2,\text{sw}} - \text{pCO}_{2,\text{air}})$$

CMIP6 models & AWI-ESM-1-REcoM

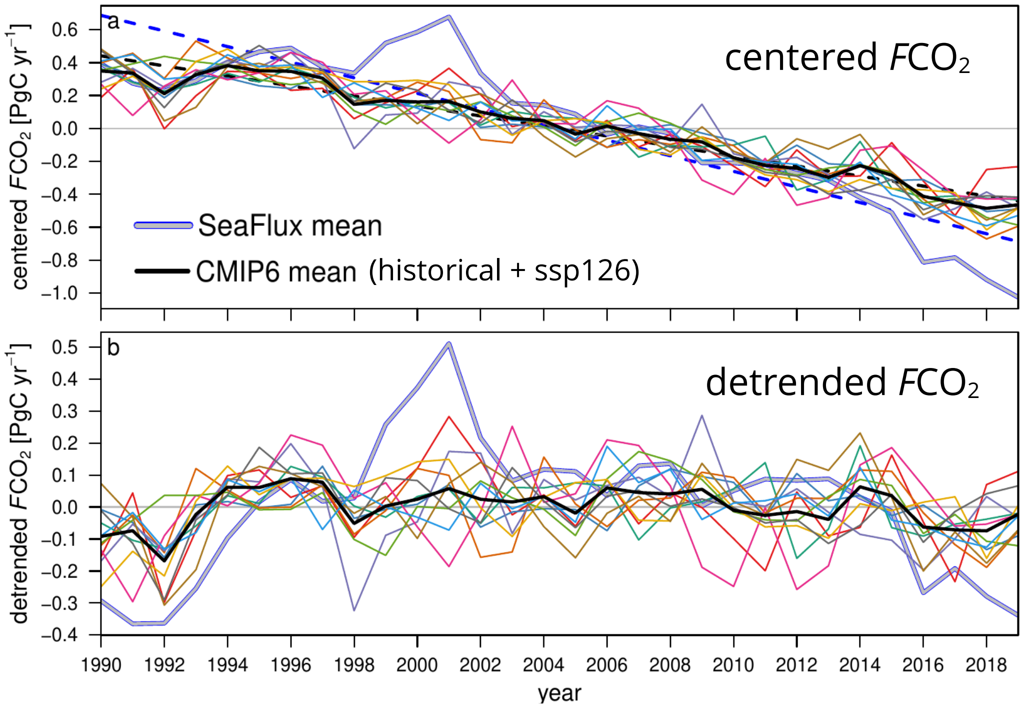

- → focus on temporal variability: center/detrend
- → FCO_2 weakening (1990s), reinvigoration (after 2000) and latest increase missing in CMIP6
- → ΔpCO2 explains FCO2; pCO2,atm is well known
- → systematic bias in pCO_2 in CMIP6 models?

ALFRED-WEGENER-INSTITUT
HELMHOLTZ-ZENTRUM FÜR POLAR- UND MEERESFORSCHUNG

Global detrended pCO_2

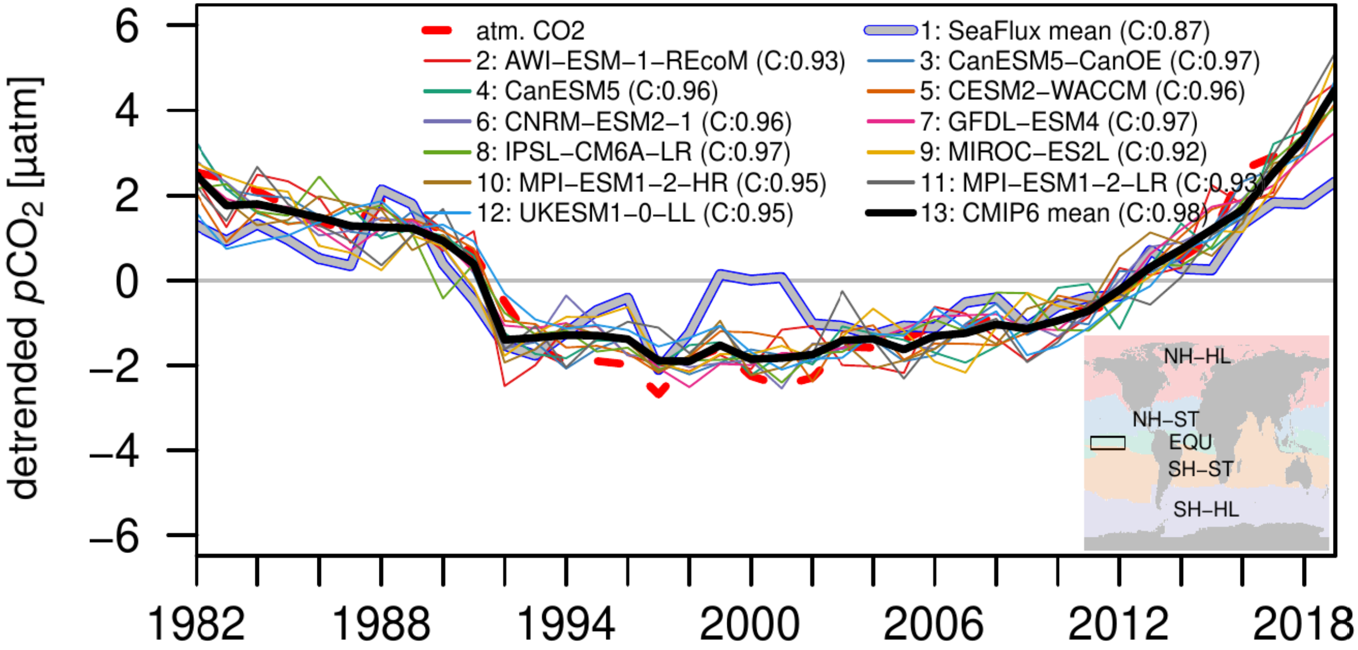

→ decadal-scale pCO_2 variability set by $CO_{2,atm}$

→ interannual variability underestimated in CMIP6 (e.g. around 2000, since 2017)

CO_2 biomes (Gregor et al. 2019)

→ models do not represent pCO_2 variability due to ENSO

→ modeled and observed SST not correlated

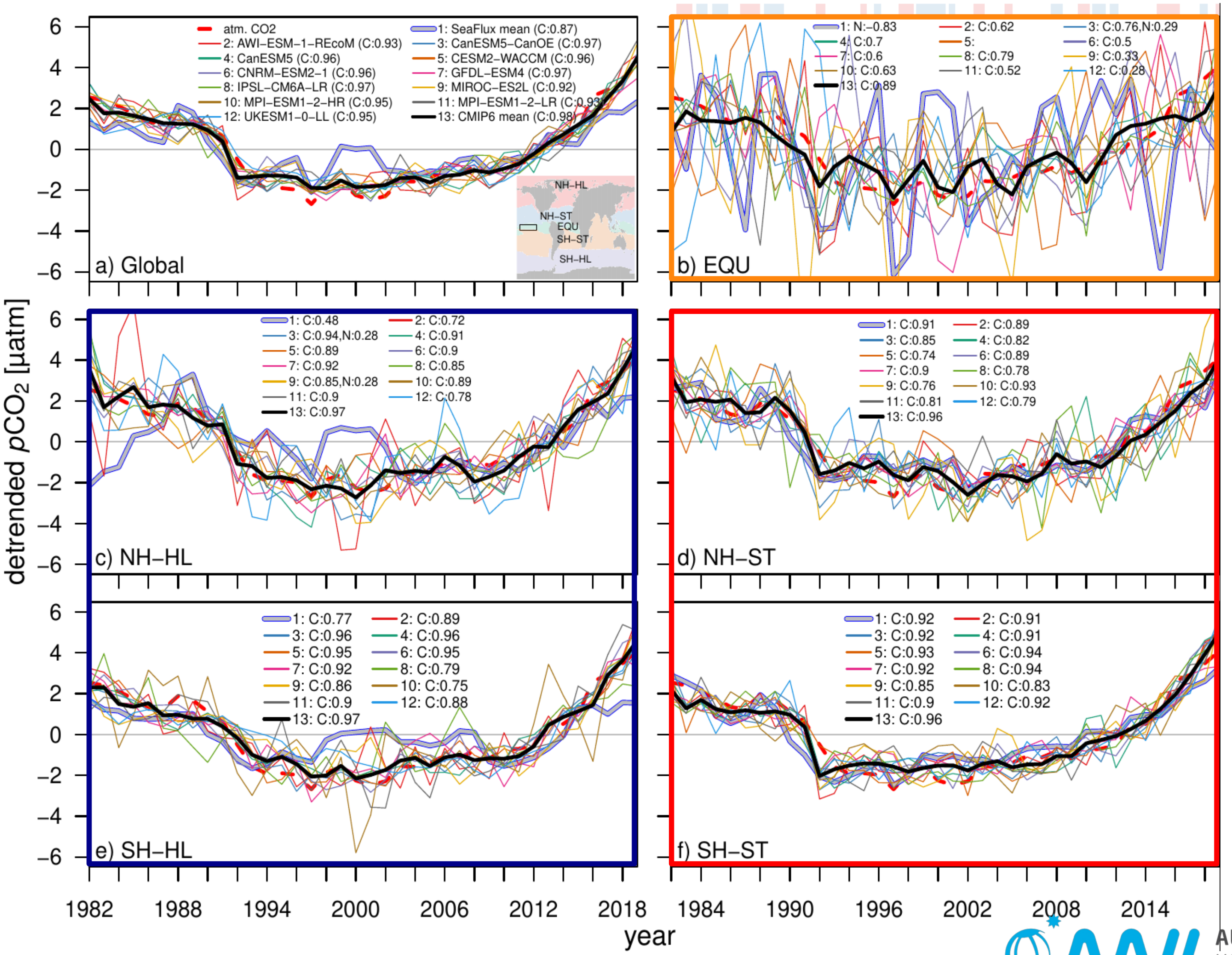

→ interannual pCO_2 variability discrepancies in high latitudes

→ models just follow $CO_{2,atm}$

→ very good model fit in subtropics

→ high correlation pCO_2 and $CO_{2,atm}$

ALFRED-WEGENER-INSTITUT
HELMHOLTZ-ZENTRUM FÜR POLAR-
UND MEERESFORSCHUNG

→ thermal and non-thermal drivers of high-latitude pCO_2 variability

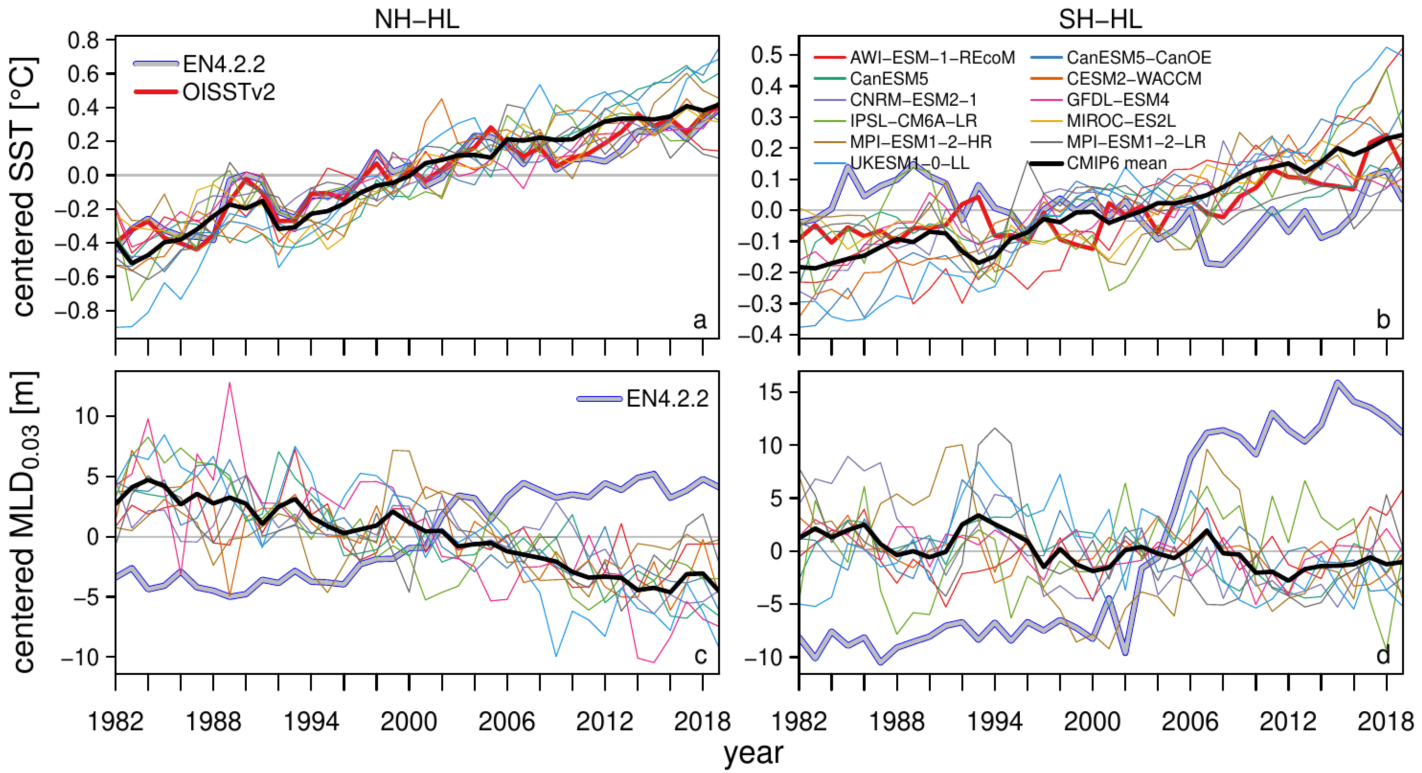

→ wrong MLD trend sign in all CMIP6 models

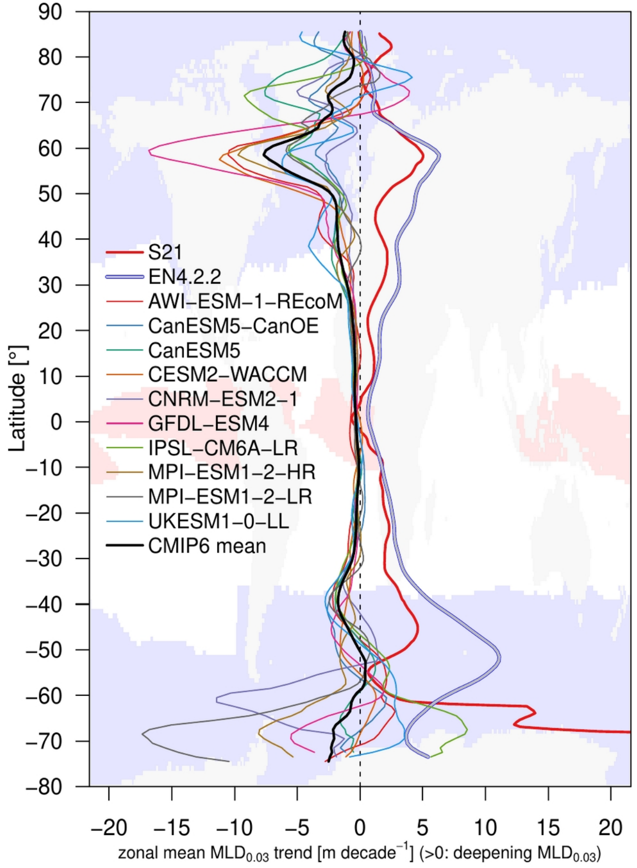

S21: Sallée et al. 2021

ALFRED-WEGENER-INSTITUT
HELMHOLTZ-ZENTRUM FÜR POLAR-
UND MEERESFORSCHUNG

density trend

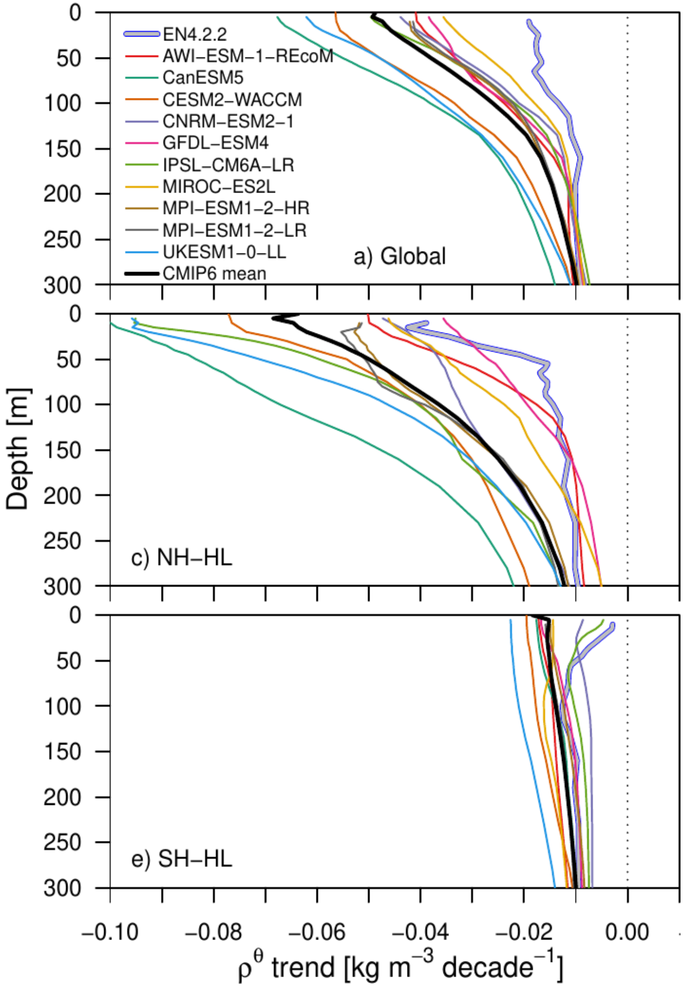

→ CMIP6 models overestimate upper ocean lightening

→ flatter density profiles

→ trend to shallower MLD, in contrast to observations

→ inhibited vertical DIC transport in high-latitudes reduces *p*CO_2 variability

→ not the case in temperature and $CO_{2,atm}$-driven subtropics

→ in line with previous work (McKinley et al. 2020, Bourgeois et al. 2022, Fu et al. 2022)

ALFRED-WEGENER-INSTITUT
HELMHOLTZ-ZENTRUM FÜR POLAR-
UND MEERESFORSCHUNG

density trend

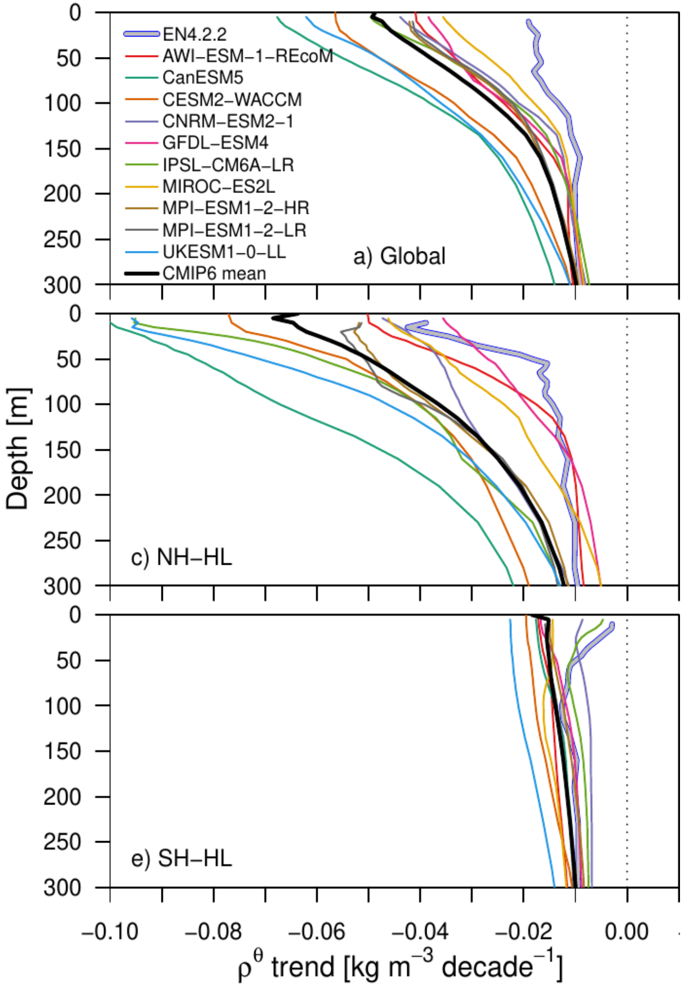

too strong $CO_{2,atm}$ forcing in models since 2017?

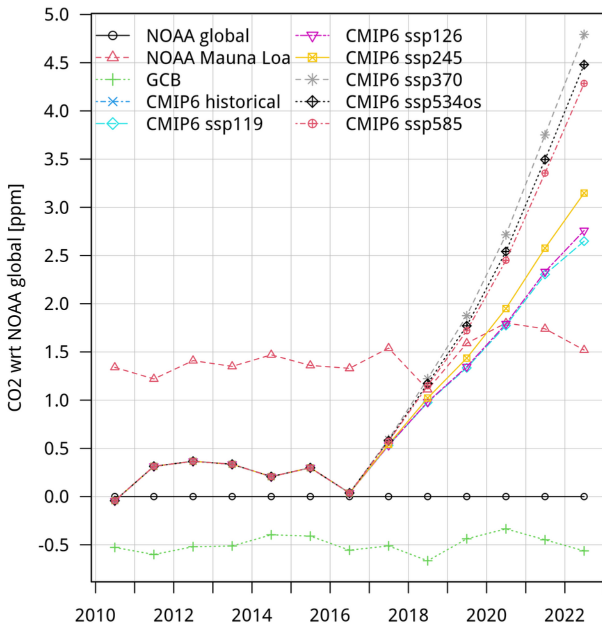

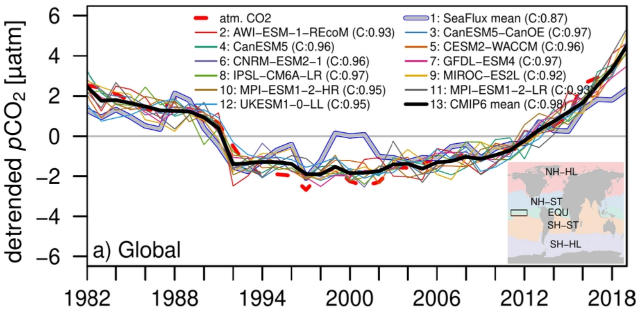

→ CMIP6 models overestimate upper ocean lightening

→ flatter density profiles

→ trend to shallower MLD, in contrast to observations

→ inhibited vertical DIC transport in high-latitudes reduces *p*CO_2 variability

→ not the case in temperature and $CO_{2,atm}$-driven subtropics

→ in line with previous work (McKinley et al. 2020, Bourgeois et al. 2022, Fu et al. 2022)

Thank you! cdanek@awi.de

(refs and paper)

ALFRED-WEGENER-INSTITUT
HELMHOLTZ-ZENTRUM FÜR POLAR- UND MEERESFORSCHUNG

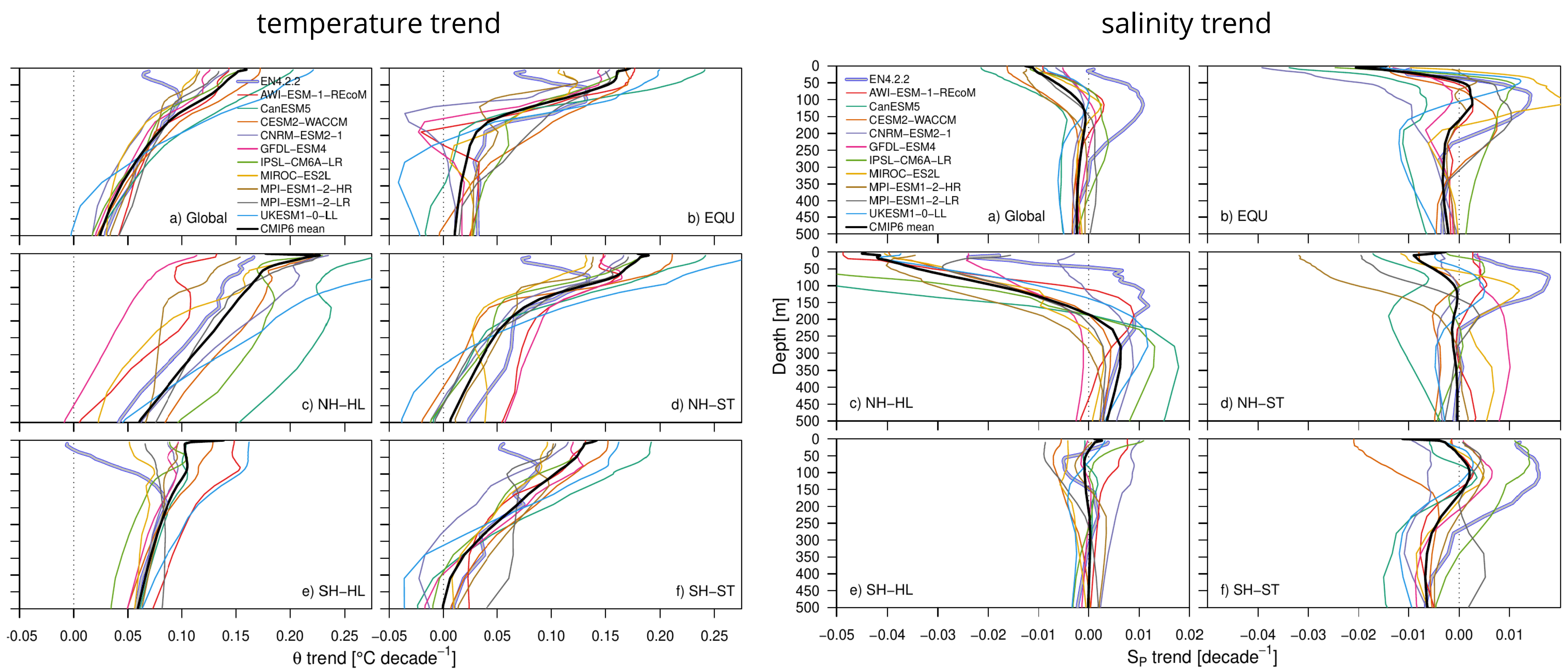

temperature trend
salinity trend
EN4.2.2
AWI−ESM−1−REcoM
CanESM5
CESM2−WACCM
CNRM−ESM2−1
GFDL−ESM4
IPSL−CM6A−LR
MIROC−ES2L
MPI−ESM1−2−HR
MPI−ESM1−2−LR
UKESM1−0−LL
CMIP6 mean
a) Global
b) EQU
c) NH−HL
d) NH−ST
e) SH−HL
f) SH−ST
θ trend [°C decade−1]
Depth [m]
SP trend [decade−1]

resolution

12 models

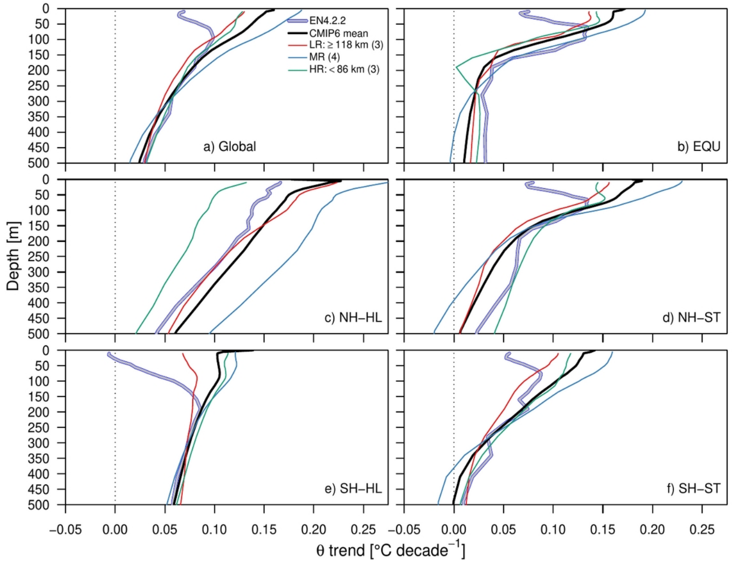

vertical

mixing

param 12

models

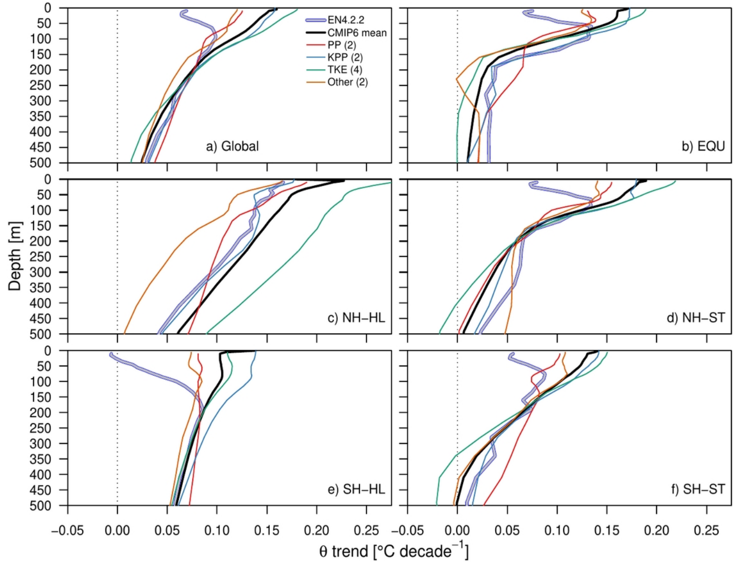

resolution

59 models

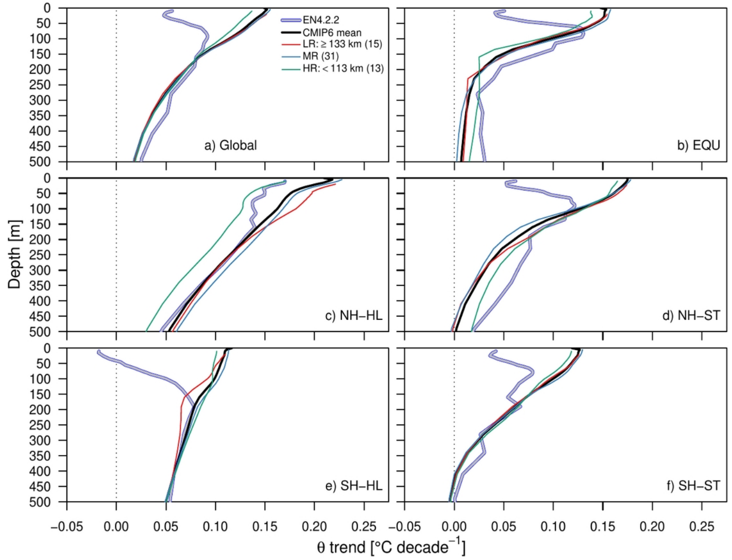

vertical

mixing

param 59

models

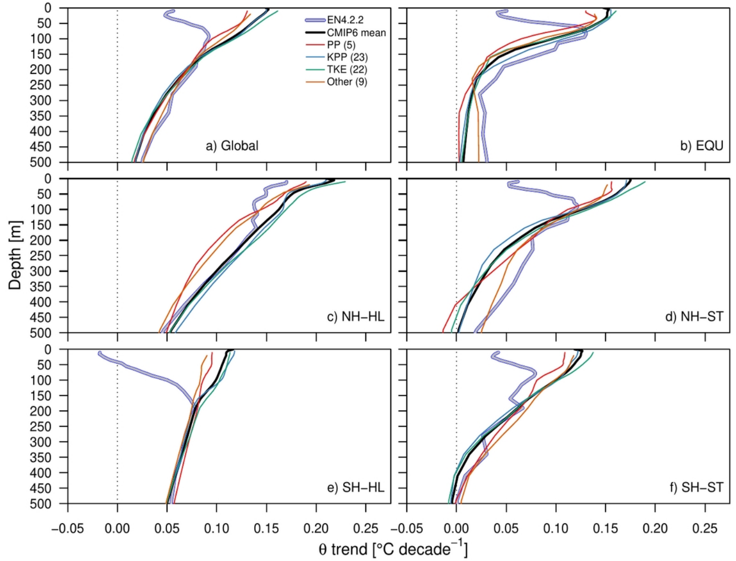

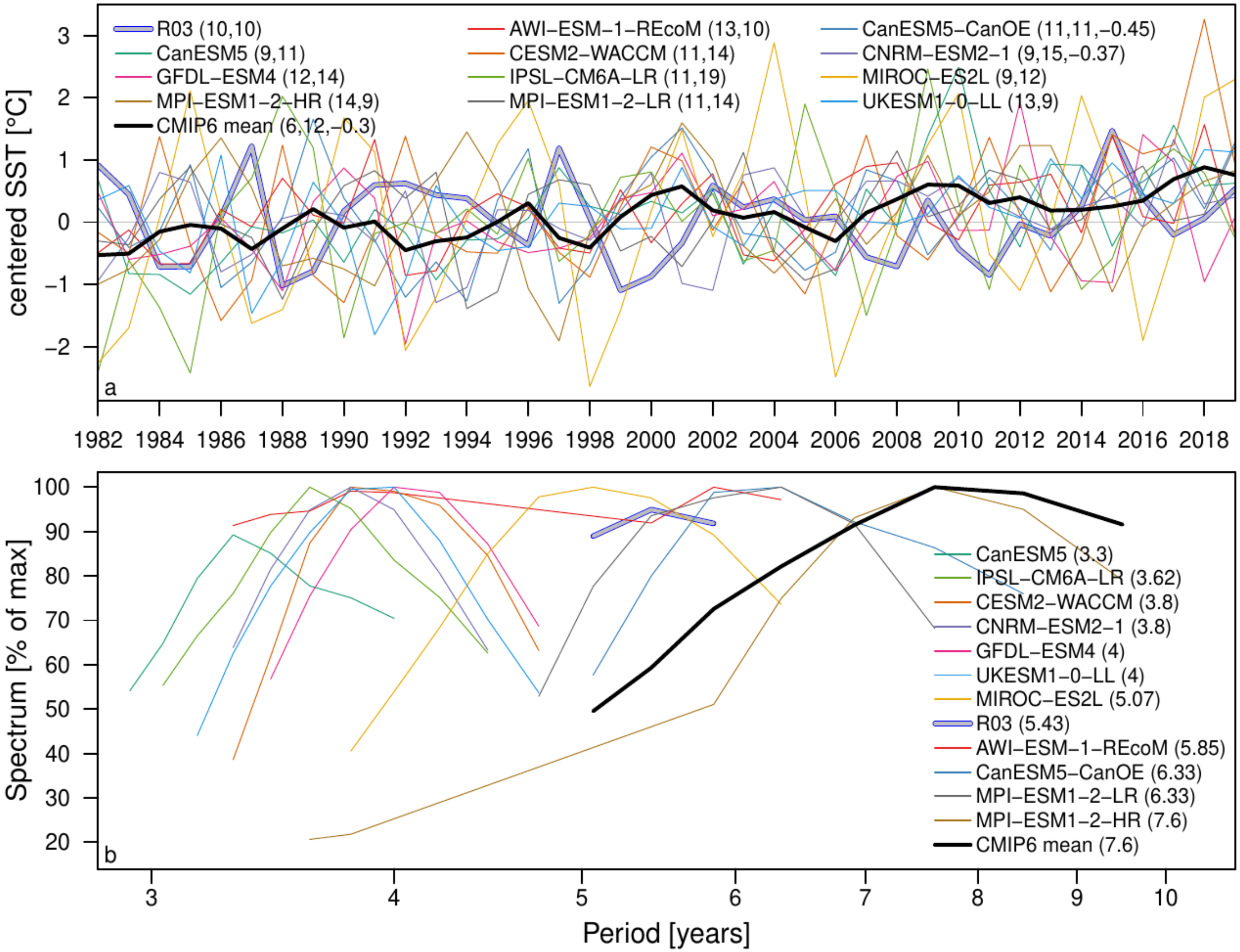

R03 (10,10)
AWI−ESM−1−REcoM (13,10)
CanESM5−CanOE (11,11,−0.45)
CanESM5 (9,11)
CESM2−WACCM (11,14)
CNRM−ESM2−1 (9,15,−0.37)
GFDL−ESM4 (12,14)
IPSL−CM6A−LR (11,19)
MIROC−ES2L (9,12)
MPI−ESM1−2−HR (14,9)
MPI−ESM1−2−LR (11,14)
UKESM1−0−LL (13,9)
CMIP6 mean (6,12,−0.3)
centered SST [°C]
a
b
Spectrum [% of max]
Period [years]
CanESM5 (3.3)
IPSL−CM6A−LR (3.62)
CESM2−WACCM (3.8)
CNRM−ESM2−1 (3.8)
GFDL−ESM4 (4)
UKESM1−0−LL (4)
MIROC−ES2L (5.07)
R03 (5.43)
AWI−ESM−1−REcoM (5.85)
CanESM5−CanOE (6.33)
MPI−ESM1−2−LR (6.33)
MPI−ESM1−2−HR (7.6)
CMIP6 mean (7.6)

Table 1: Data sets used as predictors for multi-linear regression of the SeaFlux ensemble mean FCO_2 from 1990 to 2019 (30 years; Gregor and Fay, 2021). All time series were annually averaged, spatially averaged/integrated over the same area, and detrended (temporal linear trend removed). ∂ denotes temporal difference, i.e. $\partial X(t) = X(t) - X(t-1)$ for year t.

No.	Predictor	Description and reference
1,2	$CO_{2,atm}$, $\partial CO_{2,atm}$	Atmospheric CO_2 concentration (Meinshausen et al, 2017)
3-5	$pCO_{2,atm}$, $\partial pCO_{2,atm}$, pCO_2	Atmospheric and sea surface CO_2 partial pressure (Gregor and Fay, 2021)
6	ΔpCO_2	$pCO_2 - pCO_{2,atm}$
7-10	W, W^2, W^3, W^4	Near-surface wind velocity from ERA5 (Copernicus Climate Change Service, 2019)
11,12	SST, ∂SST	Sea surface temperature SST from ERA5 (Copernicus Climate Change Service, 2019) or EN4.2.2 (Good et al, 2013)[a]
13,14	SSS, ∂SSS	Sea surface salinity SSS from EN4.2.2 (Good et al, 2013)
15,16	SIE_N, SIE_S	Northern and southern hemisphere sea ice extent (Fetterer et al, 2017)
17-20	$MLD_{0.01}$, $MLD_{0.03}$, $MLD_{0.125}$, MLD_{HT09}	Mixed layer depth (MLD) via potential density ρ^θ criteria 0.01, 0.03 and 0.125 kg m^{-3} and from density algorithm of Holte and Talley (2009), all based on EN4.2.2 (Good et al, 2013)[b]
21	N34	Niño 3.4 anomaly index (Rayner, 2003)[b]

[a] Choice of SST data set did not substantially effect the regression results (not shown).

[b] See section 2.4.

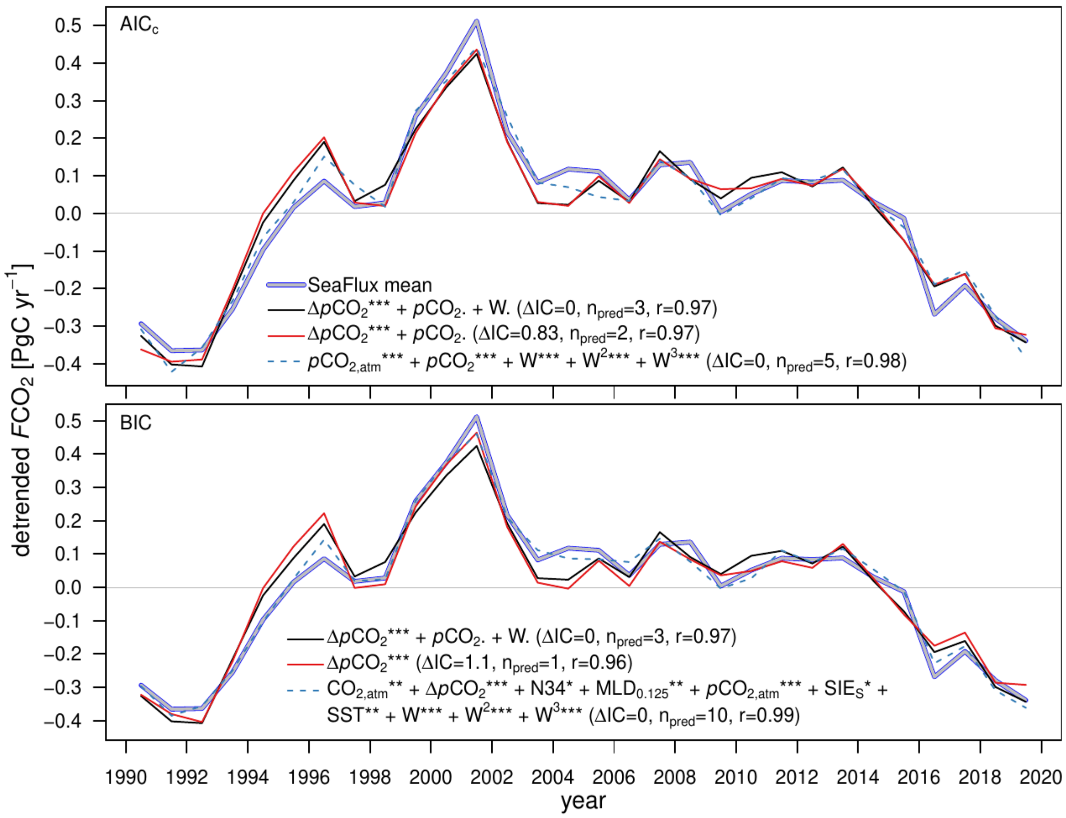

Table 2: CMIP6 ESMs analyzed in this study and their ocean model component. $\overline{d}_{\mathrm{max}}$ is the globally averaged horizontal ocean model resolution in km defined as $\sqrt{2\,A_e}$ with the surface area A_e of an irregular grid element for unstructured models (Danilov, 2022) or the maximum distance between horizontal grid cell vertices, i.e. $\sqrt{\Delta x^2 + \Delta y^2}$, for all other models (Taylor et al, 2018). n_{lev} is the number of vertical levels. The 'horizonal' and 'vertical' columns show tracer parameterizations utilized in the ocean model as identified in the given references (not meant to be complete; unstable stratification is compensated by some sort of fast and complete convection in all ocean models (Rahmstorf, 1993) and is omitted in the 'vertical' column). C87: Cox (1987), EPBL (energetic planetary boundary layer scheme): Reichl and Hallberg (2018), FFH: Fox-Kemper et al (2008), G95: Gent et al (1995), GM90: Gent and Mcwilliams (1990), KPP (k-profile parameterization): Large et al (1994), NK99: Noh and Jin Kim (1999), PP: Pacanowski and Philander (1981), R82: Redi (1982), TKE (turbulent kinetic energy scheme): Gaspar et al (1990).

No	ESM	Ocean model	$\overline{d}_{\mathrm{max}}$	n_{lev}	horizontal	vertical
1	AWI-ESM-1-REcoM (Semmler et al, 2020, this study)	FESOM1.4 (Wang et al, 2014)	76	46	R82, G95	KPP
2,3	CanESM5{-CanOE} (Swart et al, 2019)	NEMO3.4.1 (Saenko et al, 2018)	116	{41,45}	R82, GM90	TKE
4	CESM2-WACCM (Danabasoglu et al, 2020)	POP2 (Danabasoglu et al, 2012)	113	60	R82, GM90	KPP, FFH
5	CNRM-ESM2-1 (Séférian et al, 2019)	NEMO3.6 (Danabasoglu et al, 2014; Voldoire et al, 2019)	118	75	R82, GM90	TKE, FFH
6	GFDL-ESM4 (Dunne et al, 2020)	GFDL-OM4 (Adcroft et al, 2019)	59	75	R82, G95	EPBL, FFH
7	IPSL-CM6A-LR (Boucher et al, 2020)	NEMO3.6 (Boucher et al, 2020)	117	75	R82, GM90	TKE, FFH
8	MIROC-ES2L (Hajima et al, 2020)	COCO4.9 (Hasumi, 2015)	125	63	C87, GM90	NK99
9,10	MPI-ESM1-2-{HR,LR} (Mauritsen et al, 2019)	MPIOM1.63 (Marsland et al, 2003; Jungclaus et al, 2013)	{60,180}	40	R82, G95	PP, wind-driven turbulent mixing in mixed layer
11	UKESM1-0-LL (Sellar et al, 2019)	UK-GO6 (Storkey et al, 2018; Kuhlbrodt et al, 2018) based on NEMO3.6	117	75	R82, GM90	TKE